

**DOUBLE-NETWORK ALGINATE/GRAPHENE BEADS WITH ENHANCED
ALKALI/SALT RESISTANCE AND ADSORPTION PERFORMANCE
TITLE NOT TO EXCEED 200 CHARACTERS – WRITTEN IN CAPITAL LETTERS
TIMES NEW ROMAN, SIZE 12, BOLD, CENTER-ADJUSTED**

Y. Zhuang¹, F. Yu³, J. Ma^{1*}, J. Chen^{1,2*}

¹ State Key Laboratory of Pollution Control and Resource Reuse, School of Environmental Science and Engineering, Tongji University, 1239 Siping Road, Shanghai 200092, P. R. of China. Tel: 86-21-6598 1831; E-mail: jma@tongji.edu.cn

² Department of Mechanical Engineering, University of Wisconsin-Milwaukee, Milwaukee, WI 53211, USA. E-mail: jhchen@uwm.edu

³ College of Chemistry and Environmental Engineering, Shanghai Institute of Technology, Shanghai 2001418, China

Introduction

Alginate, a natural polysaccharide extracted from seaweeds, has a linear chain structure of (1–4)-linked β-D-mannuronic acid (M) and α-L-guluronic acid (G) residues arranged in a blockwise fashion, providing it with hydrophilicity, biocompatibility, nontoxicity and exceptional formability¹. Alginate chelates with divalent cations to form hydrogels. Gel formation is driven by the interactions between G-blocks, which associate to form tightly held junctions in the presence of divalent cations². The affinity of alginates towards divalent ions decreases in the following order: Pb > Cu > Cd > Ba > Sr > Ca > Co/Ni/Zn > Mn/Ca²⁺; however, it is the most commonly used cation to induce alginate gel formation. Ionic crosslinking of alginates in the presence of divalent cations is well known³. Alginate gels are widely used in a variety of areas such as biomedical area and functional materials^{4,5}; however, ionic alginate gels have limited stability, as ion exchange with monovalent ions could destabilize and rupture the gel⁶. Moreover, the use of hydrogels has been severely limited because conventional hydrogels inevitably “swell” under specific conditions, which drastically degrades their mechanical properties⁷.

Conventional methods to stabilize alginate hydrogels include covalent crosslinking and application of high concentrations of crosslinking cations to ensure tight connections between the polymer chains⁸. Halina *et al.*⁹ found that poly(vinyl alcohol) (PVAL)/GO was more photo-stable compared with PVAL alone; therefore, the addition of GO may be a solution for alginate’s weakness.

Graphene oxide (GO) is composed of planar, graphene-like, aromatic patches of random size separated by sp³-hybridized carbons. Graphene-based hydrogels can be obtained by introducing reducing agents or heat treatment during the self-assembly of GO sheets, hence the process involves reducing GO sheets and self-assembly of the reduced-GO sheets. There are numerous chemical functionalities on the sheets such as hydroxyl, epoxy, and carboxyl groups, allowing GO to be further functionalized for hybridization with other materials to form composite materials.¹⁰ GO and alginate both contain negative ions, which causes electrostatic repulsions between them and allows GO to be well dispersed¹¹. Moreover, GO nanosheets can crosslink the polymer chains of hydrogel through surface grafting and hydrogen interaction¹². Previous studies have investigated the preparation of GO and alginate^{13; 14; 15}; however, GO was loaded only on alginate rather than forming another network.

To obtain high-strength composite materials, Gong *et al.*¹⁶ reported the first double-network hydrogels, and preparing double-network hydrogels remains a popular method¹⁷. Typically, double-network gels consist of two interpenetrating polymer networks with contrasting mechanical properties. The first network is highly stretched and densely crosslinked, making it stiff and brittle; the second network is flexible and sparsely crosslinked, making it soft and stretchable. In most cases, both networks are formed by covalent bonds. Compared with non-covalent bonds, the covalent sacrificial bonds of brittle networks have the advantages of high bond energy, weak temperature dependence and the rate of deformation¹⁸.

Fan *et al.*¹² prepared a double-network nanocomposite consisting of GO, alginate and polyacrylamide, but the double network in this material was formed by alginate and polyacrylamide, while GO were only used as an additive. Sun *et al.*¹⁹ synthesized extremely stretchable and tough hydrogels by ionically crosslinked alginate

and covalently crosslinked polyacrylamide. Huang *et al.*²⁰ prepared a double-network hydrogel of graphene and poly(acrylic acid) with excellent mechanical properties. These studies show that GO and alginate are good candidates to form double networks; however, in previous studies, synthetic high-molecular polymers were the main choices for the formation of double networks, because the goal in the traditional double-network studies was to obtain gels with better mechanical properties.

In the case of GO, it could form 3D networks crosslinked by polymers, and studies have investigated the composite of graphene and natural polymers²¹; however, until now, it has not been used as one of the double networks for natural polymer. Moreover, it is worth noting that GO nanosheets could form a loose 3D network originating from the coordinating interactions between oxygen-containing groups of GO and calcium ions, which has been ignored in previous studies of GO and alginate composite. Therefore, since GO also is a crosslinker for polymers²², we prepared a double-network hydrogel consisting of GO and alginate (shown in Schem. 1) in order to provide the alginate with better stability and adsorption ability. Ca²⁺ was used in this study as an alginate crosslinker not only for its popular use in alginate gelation, but also for its coordinating interactions with GO. This study also explored the stability and structure of the double network and the methylene blue adsorption capacity of the materials.

Materials and methods

The surface morphologies of GAS and GAD (GO 8 mg/mL) were visualized using a field-emission SEM (Hitachi, S-4800) and TEM (JEOL, JEM-2010). The hydrophilicities were characterized by an optical contact angle meter (Dataphysics, OCA-20). The surface functional groups were observed by FTIR (NEXUS, 670). Measurements of micro-Raman spectra were carried out using a Raman Scope system (LabRam, 1B) with a 532 nm wavelength incident laser light and 20 mW power. The XRD were collected on a Bragg-Brentano diffractometer (Rigaku, D/Max-2200) with monochromatic Cu K α radiation ($\lambda = 1.5418 \text{ \AA}$) of a graphite curve monochromator, and the data were collected from $2\theta = 2\text{-}40^\circ$ at a continuous scan rate of $2^\circ/\text{min}$ for phase identification. The BET isotherms were measured by an Accelerated Surface Area and Porosimetry system (Micromeritics, ASAP 2020).

The adsorption isotherm was studied at pH=8 in a thermostatic shaker at 150 rpm at 298 K for 24 h under solid to liquid ratio 1 mg/mL. After adsorption, A, GAS, and GAD (GO 8 mg/mL) were separated using a 0.45 μm membrane, and the methylene blue concentrations in the solution were determined by an ultraviolet spectrophotometer (Tianmei UV-2310(II)) at 664 nm.

Results and discussion:

Fig. 1 shows an optical image of hydrogels with different GO content. It can be seen that the diameter of the beads increased with GO content rising both for the single network and double network, indicating a good combination of graphene and alginate.

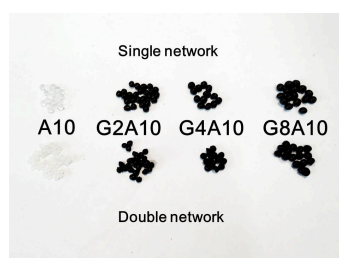


Fig. 1 Optical image of hydrogels with different GO content.

Fig. 2 shows the SEM and EDS of GAS and GAD. There are scattered bulks in GAS, as shown in Fig.2a, and there are petal-like pieces in GAD, as shown in Fig.2b.

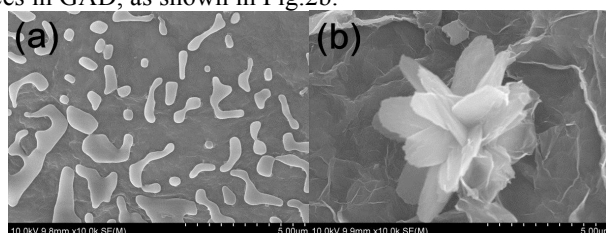


Fig.2 Microstructure. SEM of (a) G8A10-S and (b) G8A10-D.

As is known that alginate based materials have limited stability and could swell in as monovalent ions solution²³, then, the GO/alginate gels have higher swelling ratio under higher pH, to further studied the disadvantage of monovalent ions exchange and swelling, and evaluate the difference between single network and double network, we put GAS and GAD into NaOH solution of pH 13 and saturated solution of NaCl as shown in Fig.3. Under pH 13, within 5 min suspensions appeared in the solution contained GAS due in 5 min which was caused by to the over -swelling of alginate under strong base. Both GAS and GAD began to sinkgo down in 5 min, but GAD sank much more slowlyly than GADS. After 30 min, almost all the GAS beads reached the bottom of the beaker while most of the GAD beads remainedstill stayed in the upside of the solution. After 24 h, though most of the GAS beads sankgot to the bottom, the solution still remaintainedmaind clear. AsSince the beads had a higher swelling ratio under higher pH, it can be seen that the GAD had better pH tolerance ability than GAS. In a saturated solution of NaCl, the difference of the go -down speed between GAS and GAD was more obvious:. Aafter 6h, almost all of the GAS beads reached the bottom of the beaker while almost all of the GAD beads did not have visible movement. After 48 h, the GAD beads arrived at the bottom without obvious size change,, while on the opposite, the GAD beads evidently became larger. ThereforeHence, the GAD had better stability in high -concentration salt solution than GAS.

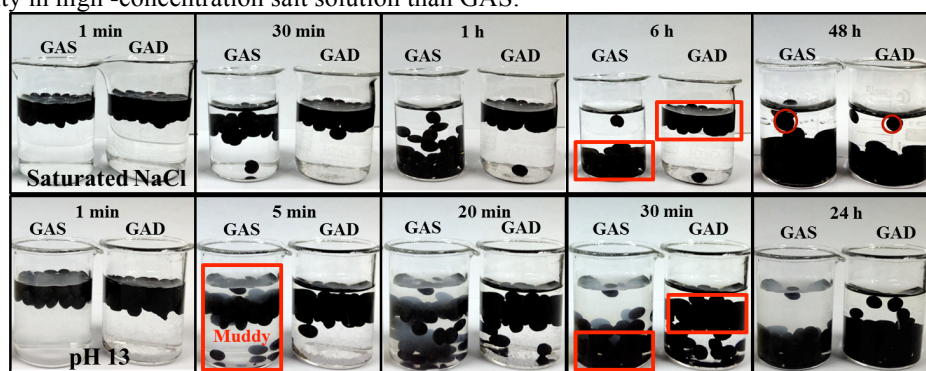


Fig.3 Photograph of G8A10-S and G8A10-D in saturated NaCl and NaOH in different time(pH 13)

Fig. 4 shows the Langmuir isotherms for methylene blue adsorption onto A, GAS, and GAD. The maximum adsorption capacities of A, GAS, and GAD for methylene blue are 0.825 g/g (R^2 0.9997), 1.971 g/g (R^2 0.9990), and 2.256 g/g (R^2 0.9957), respectively. The result further proves that nanoparticles help to improve the adsorption ability of alginate gels, which has also been proved by other studies. Moreover, the result also shows that double networks have better adsorption capacity than single networks compared with other methylene blue adsorption studies on alginate-based materials, such as magnetic alginate beads 198 mg/g²⁴, alginate-halloysite nanotube beads 250 mg/g²⁵, calcium alginate/activated carbon composite beads 892 mg/g²⁶, and alginate-g-poly(sodium acrylate-co-styrene) 1843.46 mg/g²⁷.

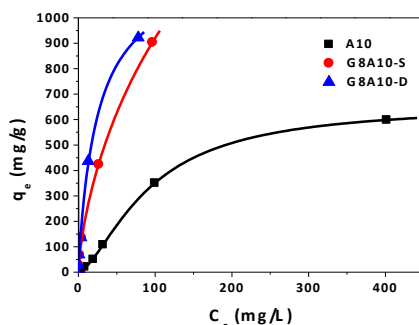


Fig. 4 Langmuir isotherms for methylene blue adsorption onto A10, G8A10-S and G8A10-D,

Acknowledgements:

This research is supported by The National Natural Science Foundation of China (51072135), Specialized Research Fund for the Doctoral Program of Higher Education (20100072110033), and Program for Young Excellent Talents at Tongji University (2010KJ026). We are also thankful to anonymous reviewers for their valuable comments to improve this manuscript.

References

1. Li, Y., Liu, F., Xia, B., Du, Q., Zhang, P., Wang, D., Wang, Z. & Xia, Y. (2010). *Journal of Hazardous Materials* **177**, 876-880.
2. Sikorski, P., Mo, F., Skjak-Braek, G. & B.T.Stokke. (2007). *Biomacromolecules* **8**, 2098-2103.
3. Morch, Y. A., Donati, I., Strand, B. L. & Skjak-Braek, G. (2006). *Biomacromolecules* **7**, 1471-1480.
4. Lee, K. Y. & Mooney, D. J. (2012). *Prog Polym Sci* **37**, 106-126.
5. Fusco, S., Sakar, M. S., Kennedy, S., Peters, C., Bottani, R., Starsich, F., Mao, A., Sotiriou, G. A., Pané, S., Pratsinis, S. E., Mooney, D. & Nelson, B. J. (2014). *Advanced Materials* **26**, 952-957.
6. Thu, B., Bruheim, P., Espevik, T., Smidsrod, O., SoonShiong, P. & SkjakBraek, G. (1996). *Biomaterials* **17**, 1069-1079.
7. Kamata, H., Akagi, Y., Y. Kayasuga-Kariya, Chung, U. & Sakai, T. (2014). *Science* **343**, 873-875.
8. Matyash, M., Despang, F., Ikonomidou, C. & Gelinsky, M. (2014). *Tissue Eng Part C Methods* **20**, 401-11.
9. Peregrino, P. P., Sales, M. J., da Silva, M. F., Soler, M. A., da Silva, L. F., Moreira, S. G. & Paterno, L. G. (2014). *Carbohydrate Polymers* **106**, 305-11.
10. Shao, J. J., Lv, W. & Yang, Q. H. (2014). *Advanced Materials* **26**, 5586-5612.
11. He, Y., Zhang, N., Gong, Q., Qiu, H., Wang, W., Liu, Y. & Gao, J. (2012). *Carbohydrate Polymers* **88**, 1100-1108.
12. Fan, J., Shi, Z., Lian, M., Li, H. & Yin, J. (2013). *Journal of Materials Chemistry A* **1**, 7433.
13. Li, Y., Du, Q., Liu, T., Sun, J., Wang, Y., Wu, S., Wang, Z., Xia, Y. & Xia, L. (2013). *Carbohydrate Polymers* **95**, 501-507.
14. Algothmi, W. M., Bandaru, N. M., Yu, Y., Shapter, J. G. & Ellis, A. V. (2013). *Journal of Colloid and Interface Science* **397**, 32-38.
15. Wu, S., Zhao, X., Li, Y., Zhao, C., Du, Q., Sun, J., Wang, Y., Peng, X., Xia, Y., Wang, Z. & Xia, L. (2013). *Chemical Engineering Journal* **230**, 389-395.
16. Gong, J. P., Kurokawa, T., Narita, T., Kagata, G., Osada, Y., Nishimura, G. & Kinjo, M. (2001). *Journal of The American Chemical Society* **123**, 5582-5583.
17. Ducrot, E., Chen, Y. L., Bulters, M., Sijbesma, R. P. & Creton, C. (2014). *Science* **344**, 186-189.
18. Gong, J. P. (2014). *Science* **344**, 161-162.
19. Sun, J. Y., Zhao, X., Illeperuma, W. R., Chaudhuri, O., Oh, K. H., Mooney, D. J., Vlassak, J. J. & Suo, Z. (2012). *Nature* **489**, 133-6.
20. Huang, P., Chen, W. & Yan, L. (2013). *Nanoscale* **5**, 6034-9.
21. Xu, Y., Wu, Q., Sun, Y., Bai, H. & Shi, G. (2010). *ACS Nano* **4**, 7358-7362.
22. Cong, H.-P., Wang, P. & Yu, S.-H. (2013). *Chemistry of Materials* **25**, 3357-3362.
23. Huang, Z., Liu, S., Zhang, B. & Wu, Q. (2014). *Carbohydrate Polymers* **113**, 430-437.
24. Rocher, V., Siaugue, J. M., Cabuil, V. & Bee, A. (2008). *Water Research* **42**, 1290-8.
25. Liu, L., Wan, Y., Xie, Y., Zhai, R., Zhang, B. & Liu, J. (2012). *Chemical Engineering Journal* **187**, 210-216.
26. Hassan, A. F., Abdel-Mohsen, A. M. & Fouda, M. M. (2014). *Carbohydrate Polymers* **102**, 192-8.
27. Wang, Y., Wang, W. & Wang, A. (2013). *Chemical Engineering Journal* **228**, 132-139.